Front. Optoelectron. China 2009, 2(1): 9–14
DOI 10.1007/s12200-008-0074-5

RESEARCH ARTICLE

# Simulation of 40 Gbit/s NRZ to RZ format conversion based on sum-frequency generation using a PPLN loop mirror

**Jian WANG (✉), Junqiang SUN, Weiwei ZHANG, Zhefeng HU**

Wuhan National Laboratory for Optoelectronics, College of Optoelectronic Science and Engineering, Huazhong University of Science and Technology, Wuhan 430074, China



**Abstract** A novel scheme of all-optical format conversion is proposed and simulated from non-return-to-zero (NRZ) to return-to-zero (RZ) at 40 Gbit/s by exploiting sum-frequency generation (SFG) in a periodically poled lithium niobate loop mirror (PPLN-LM). The conversion performance is analyzed, including eye diagrams, conversion efficiency, pulse width ratio, duty cycle, *Q*-factor, extinction ratio, and tunability. It is found that the signal wavelength can be tuned in a wide wavelength range by properly changing the pump wavelength.

**Keywords** nonlinear optics, optical communications, all-optical signal processing, all-optical format conversion, non-return-to-zero (NRZ), return-to-zero (RZ), sum-frequency generation (SFG), periodically poled lithium niobate (PPLN), loop mirror

## 1 Introduction

All-optical format conversion between non-return-to-zero (NRZ) and return-to-zero (RZ) is an important interface technology for future optical networks that employ both wavelength-division-multiplexing (WDM) and optical time-division-multiplexing (OTDM) technologies. Different schemes with impressive performance have been investigated to realize NRZ to RZ format conversion, including nonlinear optical loop mirror (NOLM) [1], dual-wavelength injection locking [2], and semiconductor optical amplifiers (SOAs) [3]. Recently, a promising approach for all-optical signal processing is to use a periodically poled lithium niobate (PPLN) waveguide for distinct advantages such as a high nonlinear coefficient, ultra-fast response, negligible spontaneous emission noise, the absence of intrinsic frequency chirp, and complete transparency to bit rate and data format [4–25]. Currently, PPLN has wide applications in wavelength conversions [5–17] and logic gates [18–22]. In this paper, by using sum-frequency generation (SFG) in a PPLN loop mirror (PPLN-LM), we propose a novel realization of 40 Gbit/s format conversion from NRZ to RZ. The eye diagrams, conversion efficiency, pulse width ratio, duty cycle, *Q*-factor, extinction ratio (ER), and tunability are simulated, showing impressive conversion performance.

Received December 7, 2007; accepted April 1, 2008
E-mail: wjhustoe@163.com

## 2 Principle of operation

The proposed PPLN-LM for NRZ to RZ format conversion is illustrated in Fig. 1. The operational principle can be briefly described as follows: the input NRZ signal is split into clockwise (CW) and counter-clockwise (CCW) signals with the same power level at ports ③ and ④ by a 3 dB fiber coupler (FC). The synchronized pump pulse trains are injected into PPLN-LM along the CW direction by a WDM FC. When the pump is off, no output signal can be obtained at port ② due to the destructive interference [1]. When the pump is on, the co-propagating CW signal and CW pump take part in the SFG nonlinear interaction inside PPLN under the quasi-phase matching (QPM) condition: one signal photon and another pump photon are annihilated to create one sum-frequency photon. Thus, within the region where the pulsed pump is present, the CW signal is depleted and notches in the output CW signal from PPLN can be found (point A in Fig. 1). On the other hand, the CCW signal and the CW pump propagate in opposite directions, and therefore cannot interact with each other effectively. Moreover, as the co-propagating CW signal and the CW pump satisfy the SFG QPM condition, the SFG process between the counter-propagating CCW signal and the CW pump is severely phase mismatched. As a result, the SFG process between the CCW signal and the CW pump can be ignored. Thus, the CCW signal experiences negligible changes and is similar to the input NRZ signal after

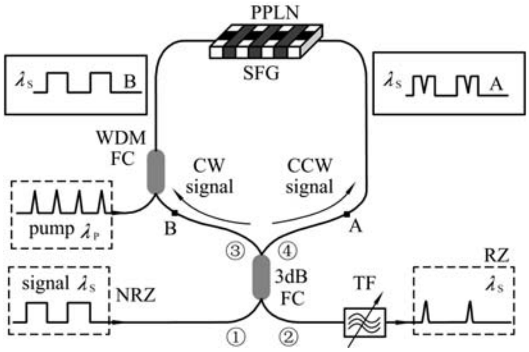


**Fig. 1** Schematic diagram of NRZ to RZ format conversion based on SFG in a PPLN-LM (TF: tunable filter)

traveling through the PPLN waveguide (point B in Fig. 1). Finally, the CW and CCW signals interfere in the 3 dB FC and generate the RZ signal at port ②. Therefore, the NRZ to RZ format conversion is implemented with the wavelength unchanged.

## 3 Theoretical model and simulation results

For the SFG process, when the signal (frequency $\omega_S$) and the pump (frequency $\omega_P$) are launched into the PPLN waveguide together, the sum-frequency wave is generated at a frequency of $\omega_{SF}$. Note that $\omega_S$, $\omega_P$ and $\omega_{SF}$ satisfy the energy conservation with the relationship of $\omega_S + \omega_P = \omega_{SF}$, which can be also expressed by $1/\lambda_S + 1/\lambda_P = 1/\lambda_{SF}$, where $\lambda_S$, $\lambda_P$ and $\lambda_{SF}$ denote the wavelengths of the signal, pump, and sum-frequency waves, respectively. Under the slowly varying envelope approximation, the complex amplitudes of signal $A_S$, pump $A_P$, and sum-frequency wave $A_{SF}$ are governed by the following coupled-mode equations [16]:

$$\frac{\partial A_S}{\partial z} + \beta_{1S}\frac{\partial A_S}{\partial t} + \frac{i}{2}\beta_{2S}\frac{\partial^2 A_S}{\partial t^2} + \frac{1}{2}\alpha_S A_S = i\omega_S \kappa_{SFG} A_P^* A_{SF} \exp(i\Delta k_{SFG} z), \quad (1)$$

$$\frac{\partial A_P}{\partial z} + \beta_{1P}\frac{\partial A_P}{\partial t} + \frac{i}{2}\beta_{2P}\frac{\partial^2 A_P}{\partial t^2} + \frac{1}{2}\alpha_P A_P = i\omega_P \kappa_{SFG} A_S^* A_{SF} \exp(i\Delta k_{SFG} z), \quad (2)$$

$$\frac{\partial A_{SF}}{\partial z} + \beta_{1SF}\frac{\partial A_{SF}}{\partial t} + \frac{i}{2}\beta_{2SF}\frac{\partial^2 A_{SF}}{\partial t^2} + \frac{1}{2}\alpha_{SF} A_{SF} = i\omega_{SF} \kappa_{SFG} A_S A_P \exp(-i\Delta k_{SFG} z), \quad (3)$$

$$\kappa_{SFG} = d_{eff}\sqrt{\frac{2\mu_0}{c n_S n_P n_{SF} A_{eff}}}, \quad (4)$$

$$\Delta k_{SFG} = k_{SF} - k_S - k_P - \frac{2\pi}{\Lambda}, \quad (5)$$

where $\beta_{1j}$ and $\beta_{2j}$ are, respectively, the first and second derivatives of the propagation constant $k_j$ with respect to the angular frequency $\omega$, evaluated at $\omega_j$ ($j$ = S, P, SF). $\alpha_j$ ($j$ = S, P, SF) are the loss coefficients of the PPLN waveguide. $\kappa_{SFG}$ is the coupling coefficient for the SFG process. $d_{eff}$ is the effective nonlinear coefficient. $A_{eff}$ is the effective interaction area. $n_j$ ($j$ = S, P, SF) are the refractive indexes for different optical waves. The parameter $\mu_0$ is the permeability and $c$ is the light velocity in vacuum. $\Delta k_{SFG}$ denotes the phase mismatch for the SFG process, while $\Lambda$ is the period of the periodically poled structure in the PPLN waveguide. The above coupled-mode Eqs. (1)–(3) can be numerically solved by using the finite difference beam propagation method (FD-BPM) [16,17].

In the following numerical simulations of NRZ to RZ format conversion, a 4-cm-long PPLN waveguide with an 18.8 μm microdomain period is assumed. Waveguide propagation losses of 0.35 dB/cm in the 1.5 μm band and 0.70 dB/cm in the 0.77 μm band are considered, i.e., $\alpha_S = \alpha_P$ = 0.35 dB/cm and $\alpha_{SF}$ = 0.70 dB/cm. The input NRZ signal is considered as a super-Gaussian type, $2^7$–1, 40 Gbit/s pseudorandom bit sequence (PRBS) data stream with a 30 dB extinction ratio. The synchronized pulsed pump is assumed to be a 40 GHz hyperbolic-secant pulse train with a 5.0 ps pulse width. The signal and the pump wavelengths are set at 1550.0 and 1538.0 nm respectively, generating the sum-frequency wavelength at 772.0 nm by SFG under the QPM condition ($\Delta k_{SFG} = 0$). The peak powers of input signal and pump are set at 200 and 100 mW, respectively. To evaluate the conversion performance, $Q$-factor and ER defined as $Q = 20\lg[(\mu_1 - \mu_0)/(\sigma_1 + \sigma_0)]$ and $\mathrm{ER} = 10\lg(\mu_1/\mu_0)$ are used, where $\mu_1$ and $\mu_0$ are the average power of logical '1' and '0' of the eye diagrams at the sampling time, and $\sigma_1$ and $\sigma_0$ are the corresponding standard deviations.

Figures 2(a) and 2(b) show sample 20-bit sequences of the input NRZ signal and the synchronized pump pulse train, respectively. After the SFG process, notches are observed in the CW signal at the output of PPLN as seen from Fig. 2(c), which is in accord with those shown in Fig. 1 (point A). Conversely, the output CCW signal from PPLN shown in Fig. 2(d) resembles the input NRZ signal (point B in Fig. 1). Figure 2(e) clearly shows the output RZ signal at port ② of PPLN-LM. The peak power of RZ signal is calculated at about 4.8 mW. Thus, the corresponding conversion efficiency defined as the peak power ratio of the output RZ signal to the input NRZ signal is estimated to be –16.23 dB.

Figure 3 further illustrates the eye diagrams of input NRZ signal, pump pulse train, output RZ signal, and referenced RZ signal. The nice eye opening, high $Q$-factor

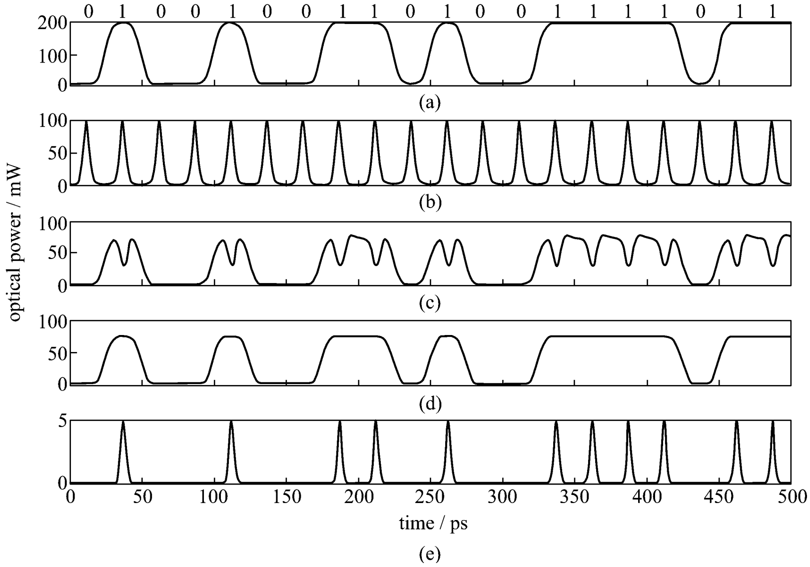


**Fig. 2** Temporal waveforms for different optical waves. (a) Input NRZ signal ($\lambda_S$); (b) input pump pulse train ($\lambda_P$); (c) output CW signal from PPLN; (d) output CCW signal from PPLN; (e) output RZ signal ($\lambda_S$) at port ② of PPLN-LM

and ER shown in Fig. 3(c) exhibit an impressive conversion performance. The pulse width of output RZ signal is about 3.52 ps, which is compressed in comparison to the input pump pulse train. The pulse width ratio of the output RZ signal to the input pulsed pump is about 0.70. The duty cycle of the output RZ signal is calculated at approximately 0.14. Figure 4 displays the optical spectra for different optical waves. Note that by comparing the eye diagrams and optical spectra of the output RZ signal shown in Figs. 3(c) and 4(c) with the referenced RZ signal shown in Figs. 3(d) and 4(d), it can be concluded that NRZ to RZ format conversion is successfully implemented with the wavelength unchanged.

Figure 5(a) depicts the dependence of conversion efficiency on the waveguide length. It is found that the efficiency increases with an increase in the length of the

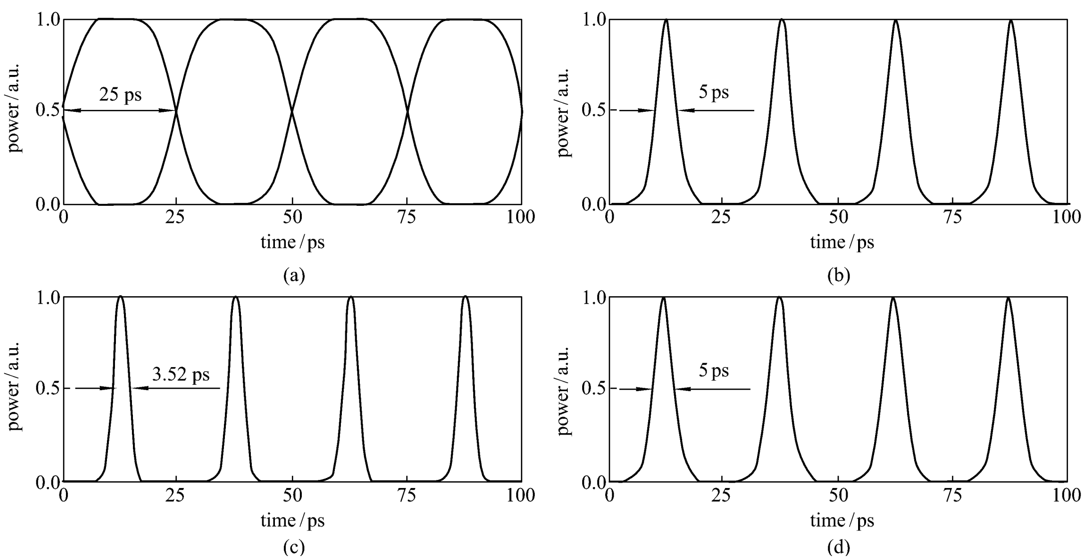


**Fig. 3** Eye diagrams for different optical waves. (a) Input NRZ signal; (b) input pump pulse train; (c) output RZ signal ($Q$ = 46.6 dB; ER = 23.1 dB); (d) referenced $2^7$–1, 40 Gbit/s PRBS RZ signal of hyperbolic-secant type with a pulse width of 5 ps

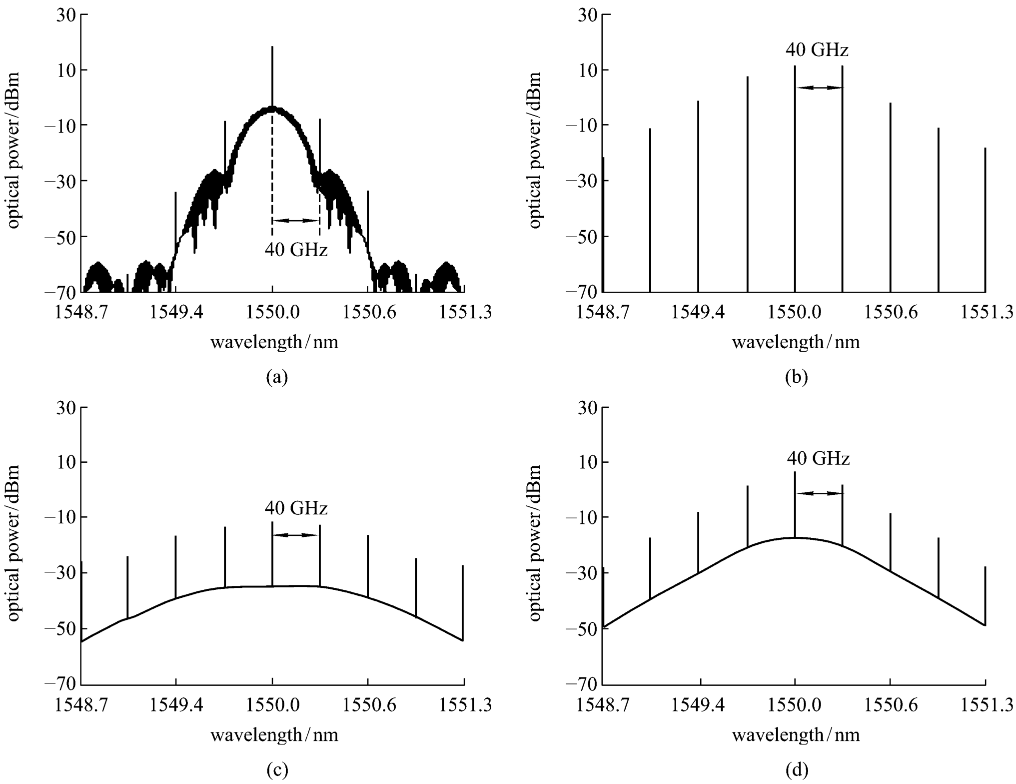


**Fig. 4** Optical spectra for different optical waves. (a) Input NRZ signal; (b) input pump pulse train; (c) output RZ signal; (d) referenced $2^7$–1, 40 Gbit/s PRBS RZ signal of hyperbolic-secant type with a pulse width of 5 ps

PPLN waveguide. Figure 5(b) presents the $Q$-factor and ER for the output RZ signal as a function of the waveguide length. It is obvious that the $Q$-factor and ER decrease with an increase in the waveguide length. Such phenomenon can be ascribed to the walk-off effect during the SFG process due to group velocity mismatch (GVM) between the signal, pump in the 1.5-μm band and sum-frequency wave in the 0.77-μm band. The longer the PPLN waveguide, the more severe the walk-off effect. Thus, the worse the conversion performance achieved with lower values of $Q$-factor and ER. Figures 5(c) and 5(d) plot the tunable performance for NRZ to RZ format conversion. To keep the SFG process quasi-phase matched ($\Delta k_{\mathrm{SFG}} = 0$) or slightly phase mismatched ($\Delta k_{\mathrm{SFG}} \approx 0$), the pump wavelength should be appropriately adjusted when changing the signal wavelength. Note that the sum-frequency wavelength is fixed at 772.0 nm in Figs. 5(c) and 5(d). It can be seen from Fig. 5(c) that the signal wavelength can be tuned widely with a 3-dB bandwidth of 105.5 nm. As shown in Fig. 5(d), the signal wavelength can be changed in a wide wavelength range of 64.0 nm with 3-dB $Q$-factor penalty and 90.5 nm with 3-dB ER penalty. Therefore, Figs. 5(c) and 5(d) show flexible NRZ to RZ format conversion with high tunability.

Remarkably, compared with other fiber loop mirrors which require precise location of the phase-shifting element inside the loop, the proposed PPLN-LM structure offers an advantage that the PPLN waveguide inside the loop can be made arbitrary. In addition, with the same PPLN-LM structure, all-optical format conversion from NRZ to RZ can also be potentially performed by using some other nonlinear interactions such as cascaded sum- and difference-frequency generation (cSFG/DFG) [24], cascaded second-harmonic generation and difference-frequency generation (cSHG/DFG) [25].

## 4 Conclusion

We have proposed and simulated a novel scheme of 40 Gbit/s NRZ to RZ format conversion by using SFG in a PPLN waveguide incorporated in a loop mirror. The eye diagrams, conversion efficiency, pulse width ratio, $Q$-factor, ER, and tunability are calculated and analyzed, showing impressive conversion performance. With further improvement, PPLN-based format conversions between various modulation formats are set to be investigated. They may have potential for future high-speed all-optical signal processing applications.

**Acknowledgements** This work was supported by the National Natural Science Foundation of China (Grant No. 60577006) and the Program for New

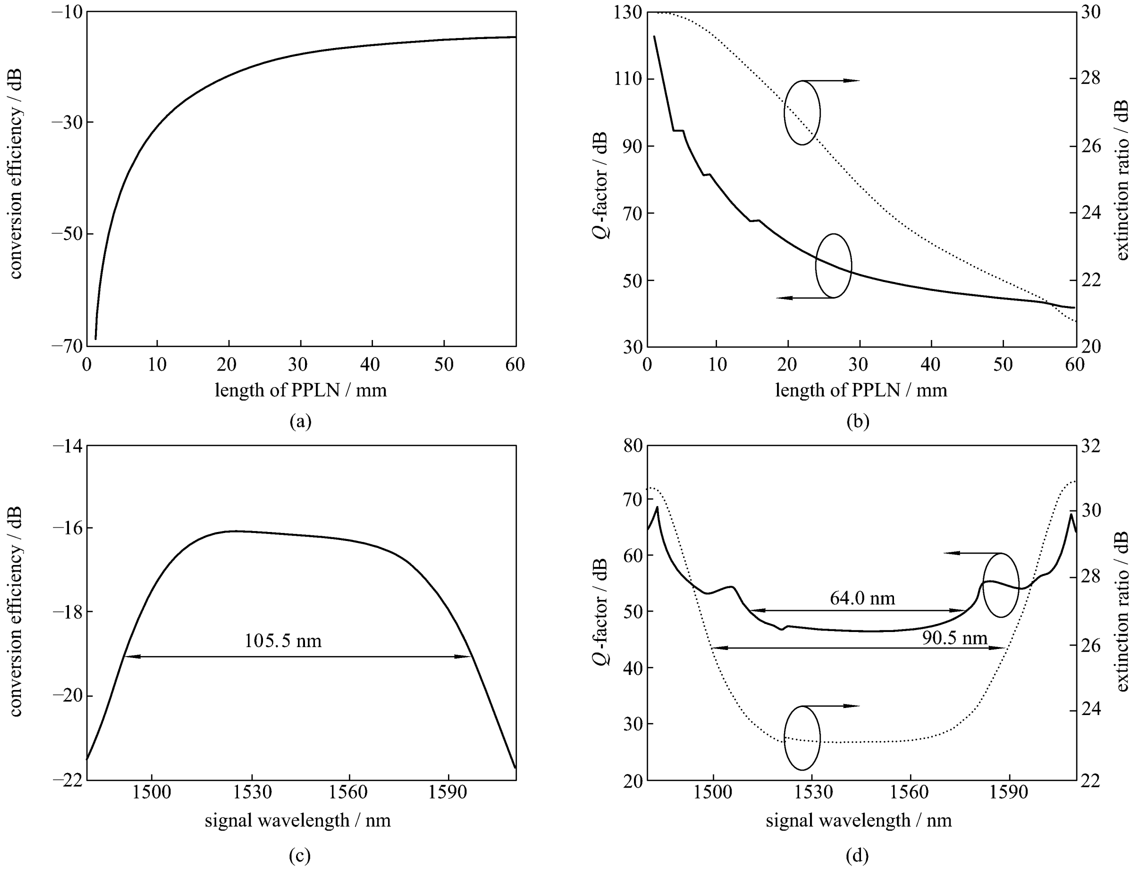


**Fig. 5** Conversion performance of NRZ to RZ format conversion based on SFG in a PPLN-LM. (a) Dependence of conversion efficiency on the length of PPLN; (b) dependence of *Q*-factor and ER on the length of PPLN; (c) dependence of conversion efficiency on the signal wavelength; (d) dependence of *Q*-factor and ER on the signal wavelength (The sum-frequency wavelength is kept at 772.0 nm for (c) and (d))

Century Excellent Talents in University, Ministry of Education of China (Grant No. NCET-04-0694).

## References

1. Bigo S, Desurvire E, Gauchard S, et al. Bit-rate enhancement through optical NRZ-to-RZ conversion and passive time-division multiplexing for soliton transmission systems. Electronics Letters, 1994, 30(12): 984–985
2. Chow C W, Wong C S, Tsang H K. All-optical NRZ to RZ format and wavelength converter by dual-wavelength injection locking. Optics Communications, 2002, 209(4–6): 329–334
3. Xu L, Wang B C, Baby V, et al. All-optical data format conversion between RZ and NRZ based on a Mach–Zehnder interferometric wavelength converter. IEEE Photonics Technology Letters, 2003, 15(2): 308–310
4. Langrock C, Kumar S, McGeehan J E, et al. All-optical signal processing using $\chi^{(2)}$ nonlinearities in guided-wave devices. Journal of Lightwave Technology, 2006, 24(7): 2579–2592
5. Xu C Q, Okayama H, Kawahara M. 1.5 μm band efficient broadband wavelength conversion by difference frequency generation in a periodically domain-inverted $LiNbO_3$ channel waveguide. Applied Physics Letters, 1993, 63(26): 3559–3561
6. Chou M H, Brener I, Fejer M M, et al. 1.5-μm-band wavelength conversion based on cascaded second-order nonlinearity in $LiNbO_3$ waveguides. IEEE Photonics Technology Letters, 1999, 11(6): 653–655
7. Xu C Q, Bracken J, Chen B. Intracavity wavelength conversions employing a MgO-doped $LiNbO_3$ quasi-phase-matched waveguide and an erbium-doped fiber amplifier. Journal of the Optical Society of America B–Optical Physics, 2003, 20(10): 2142–2149
8. Min Y H, Lee J H, Lee Y L, et al. Tunable all-optical wavelength conversion of 5ps pulses by cascaded sum- and difference frequency generation (cSFG/DFG) in a Ti:PPLN waveguide. In: Tech Dig OFC'03, 2003, 2: 767–768
9. Xu C Q, Chen B. Cascaded wavelength conversions based on sum-frequency generation and difference-frequency generation. Optics Letters, 2004, 29(3): 292–294
10. Yu S, Gu W. Wavelength conversions in quasi-phase matched $LiNbO_3$ waveguide based on double-pass cascaded $\chi^{(2)}$ SFG + DFG interactions. IEEE Journal of Quantum Electronics, 2004, 40(11): 1548–1554
11. Lee Y L, Yu B-A, Jung C, et al. All-optical wavelength conversion and tuning by the cascaded sum- and difference frequency generation (cSFG/DFG) in a temperature gradient controlled Ti:PPLN channel waveguide. Optics Express, 2005, 13(8): 2988–2993
12. Wang Jian, Sun Junqiang, Luo Chuanhong, et al. Experimental demonstration of wavelength conversion between ps-pulses based on cascaded sum- and difference frequency generation (SFG + DFG) in $LiNbO_3$ waveguides. Optics Express, 2005, 13(19): 7405–7414

13. Wang Jian, Sun Junqiang, Kurz J R, et al. Tunable wavelength conversion of ps-pulses exploiting cascaded sum- and difference frequency generation in a PPLN-fiber ring laser. IEEE Photonics Technology Letters, 2006, 18(20): 2093–2095
14. Wang Jian, Sun Junqiang, Luo Chuanhong, et al. Flexible all-optical wavelength conversions of 1.57-ps pulses exploiting cascaded sum- and difference frequency generation (cSFG/DFG) in a PPLN waveguide. Applied Physics B–Lasers and Optics, 2006, 83(4): 543–548
15. Wang Jian, Sun Junqiang. Observation of 40-Gbit/s tunable wavelength down- and up-conversions based on cascaded second-order nonlinearity in $LiNbO_3$ waveguides. Optical Engineering, 2007, 46(2): 025005
16. Wang Jian, Sun Junqiang, Zhang Xinliang, et al. Experimental observation of tunable wavelength down- and up-conversions of ultra-short pulses in a periodically poled $LiNbO_3$ waveguide. Optics Communications, 2007, 269(1): 179–187
17. Sun Junqiang, Huang Dexiu, Liu Deming. Simultaneous wavelength conversion and pulse compression exploiting cascaded second-order nonlinear processes in $LiNbO_3$ waveguides. Optics Communications, 2006, 259(1): 321–327
18. Wang Jian, Sun Junqiang, Sun Qizhen. Experimental observation of a 1.5 μm band wavelength conversion and logic NOT gate at 40 Gbit/s based on sum-frequency generation. Optics Letters, 2006, 31(11): 1711–1713
19. Wang Jian, Sun Junqiang, Sun Qizhen. Single-PPLN-based simultaneous half-adder, half-subtracter, and OR logic gate: proposal and simulation. Optics Express, 2007, 15(4): 1690–1699
20. Wang Jian, Sun Junqiang, Sun Qizhen. Proposal for all-optical switchable OR/XOR logic gates using sum-frequency generation. IEEE Photonics Technology Letters, 2007, 19(8): 541–543
21. Sun Junqiang, Wang Jian. Simulation of optical NOT gate switching by sum-frequency generation in $LiNbO_3$ waveguides. Optics Communications, 2006, 267(1): 187–192
22. Lee Y L, Yu B-A, Eom T J, et al. All-optical AND and NAND gates based on cascaded second-order nonlinear processes in a Ti-diffused periodically poled $LiNbO_3$ waveguide. Optics Express, 2006, 14(7): 2776–2782
23. Wang Jian, Sun Junqiang. NOLM-based all-optical 40 Gbit/s format conversion through sum-frequency generation (SFG) in a PPLN waveguide. In: Proceedings of SPIE, 2005, 6021: 60212H
24. Wang Jian, Sun Junqiang, Sun Qizhen, et al. Proposal and simulation of all-optical NRZ-to-RZ format conversion using cascaded sum- and difference-frequency generation. Optics Express, 2007, 15(2): 583–588
25. Wang Jian, Sun Junqiang, Sun Qizhen. Proposal for all-optical format conversion based on a periodically poled lithium niobate loop mirror. Optics Letters, 2007, 32(11): 1477–1479